HUNGARIAN UNIVERSITY OF AGRICULTURE AND LIFE SCIENCES

Modelling and performance optimization of solar drying chamber used for agricultural products

PhD Thesis

by

Halefom Kidane Abrha

Gödöllő
2025

Doctoral school

Denomination: Doctoral School of Mechanical Engineering

Science: Mechanical Engineering

Leader: Prof. Dr. Gábor Kalácska, DSc
Institute of Technology
Hungarian University of Agriculture and Life Sciences,
Gödöllő, Hungary

Supervisor: Prof. Dr. István Farkas, DSc
Institute of Technology
Hungarian University of Agriculture and Life Sciences,
Gödöllő, Hungary

Co-Supervisor: Dr. János Buzás, PhD
Institute of Technology
Hungarian University of Agriculture and Life Sciences,
Gödöllő, Hungary

…… ……

Affirmation of supervisors Affirmation of head of school

CONTENTS

1. INTRODUCTION, OBJECTIVES

Drying is a traditional and widely used method for preserving food, which extends shelf life, enhances stability, and prevents microbial growth by reducing moisture content. Despite its benefits, drying is energy-intensive and contributes significantly to overall energy consumption in many countries. To address these drawbacks, solar energy is increasingly being considered a sustainable alternative. Solar drying offers environmental and economic advantages, such as reducing greenhouse gas emissions, decreasing reliance on fossil fuels, and lowering costs for farmers especially in rural areas. With growing affordability and technological improvements, solar energy is becoming a promising solution for more sustainable agricultural practices.

Even though solar dryers are cost-effective and environmentally friendly, their overall performance still requires further investigation. The main challenges in current drying systems include poor drying uniformity, suboptimal dryer designs, and a lack of comprehensive optimization. More research is needed to address these issues and improve the efficiency and consistency of solar drying technologies.

This thesis focuses on the mathematical modelling of drying chambers and apple slices and assess the enhancement of flow uniformity mechanism within drying chambers. The challenge of uneven air distribution is well-documented in both the existing literature and practical applications, including dryers developed by previous students in Hungarian University of Agriculture and Life Sciences, Solar Energy Laboratory.

The specific objectives of this research are:

- To conduct a comprehensive thermodynamic performance analysis of the drying system.
- To enhance the airflow distribution within the drying system for better quality and effective drying of agricultural products.
- To investigate the drying kinetics and select a suitable mathematical drying model which describes the drying behaviour of apple slices.
- To study the effect of tray spacing and number of trays on the performance of the solar drying chamber.
- To identify the most influential operational parameters/variables affecting drying system performance.
- To evaluate the economic feasibility and cost-effectiveness of the solar drying system for agricultural products.

2. MATERIALS AND METHODS

This chapter offers an in-depth review of the fundamental principles of drying and related theories, with a focus on solar dryers and their classifications for agricultural preservation. It covers thin-layer models and delves into energy and exergy analysis to assess the efficiency of drying systems. Additionally, the chapter explores numerical modelling through computational fluid dynamics, highlights, optimization methods and economic analysis of drying systems.

2.1. Computational analysis

The numerical approach began with computational modelling of an existing drying chamber design that served as the foundation for this study. computational fluid dynamics analysis was used to thoroughly examine airflow patterns, heat distribution characteristics, and moisture removal efficiency within the chamber. The mesh quality was evaluated using mesh quality indicators such as skewness, aspect ratio and orthogonal quality. All mesh quality parameters met or exceeded recommended standards: skewness (0.21; ideal: 0–0.25), aspect ratio (1.8; limit: <5), and orthogonal quality (0.85; ideal: 1.0). This ensures high-fidelity simulation outcomes.

Through comprehensive *CFD* evaluation of over ten design iterations, four representative configurations, as shown in Fig. 1, were identified. Among these, and finally two chamber geometries with high air flow were selected. These selected dryers were fabricated and experiment were conducted as shown in Fig. 2. The simulation results were rigorously validated against experimental measurements using standard statistical metrics to confirm the accuracy and reliability of the computational approach.

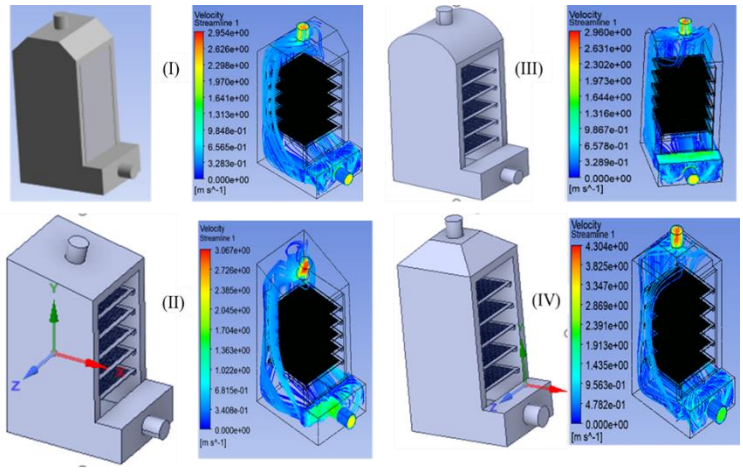

Fig. 1. Selected models with CFD streamline results

2.2. Experimental setup and procedure

This section outlines the experimental procedures used to achieve the research objectives. The same collectors were utilized across all experiments, with specific modifications made for each experiment to align with the thesis objectives.

The experimental setup comprises several key components designed for efficient solar drying (see Fig. 2). The solar air heater (SAH) features dimensions of 1.25 m × 0.5 m and includes a single-glazed configuration with a diffuser at the inlet and a circular outlet measuring 0.1 m in diameter. The drying chamber was constructed from extruded polystyrene (XPS) panels, 5 cm thick, with a thermal conductivity of 0.033 W/m.K and has internal dimensions of 1 m in height, 0.5 m in width, and 0.65 m in length. Inside the chamber, fiberglass mesh trays measuring 48 cm × 50 cm are arranged with 10 cm spacing between them to facilitate air circulation; a total of four trays were used.

Fig. 2. The setup of the drying system

2.2.1. Performance analysis of the solar drying chamber

Three experimental tests unloading (no load), half-load, and full-load were conducted to evaluate the performance of the solar dryer. The energy performance of the system was analysed using energy and exergy analysis and additional metrices like specific heat energy consumption and specific moisture extraction rate were also used to assess energy effectiveness. Exergy inflows, outflows, and losses were quantified to compute exergy efficiency, offering a comprehensive evaluation of thermodynamic performance. Key drying parameters such as drying rate, moisture content, and moisture ratio were analysed to characterize drying behaviour.

2.2.2. Mathematical modelling of applying samples

In this study, ten mathematical models were employed to describe and analyse the drying behaviour of apples. These models included the Newton, Page, Modified Page, Henderson and Pabis, Logarithmic, Two-term, Two-term exponential, Wang and Singh, Midilli and Kucuk, and Weibull distribution models. Model performance was assessed using standard statistical metrics such as the coefficient of determination (R^2), root mean square error (RMSE), and chi-square (χ^2).

2.2.3. Flow uniformity enhancement investigation

To address non flow uniformity these issues, a combination of flow-modifying devices including rectangular baffles (RB), triangular baffles (TB), and a swirler (SW) were implemented as depicted in Fig. 3. To evaluate uniformity, statistical measures including the mean, variance, standard deviation (σ), and coefficient of variation (Cv) were employed.

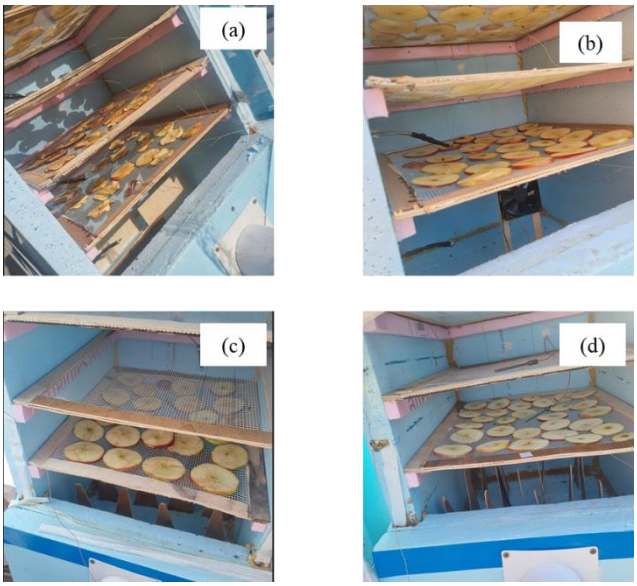

Fig. 3. Flow enhancement materials integrated within the drying chamber: rectangular baffles (a), swirler (b) and triangular baffles (c, d)

2.2.4. Effect of different operational parameters/variables

To determine the optimal configuration for these components, a Taguchi experimental design was employed.

In this study, four key control parameters were selected: solar radiation (SR), ambient temperature (T_{am}), inlet temperature of the dryer (T_{in}), and the

enhancement configuration (Type-C) of the drying chamber. The configurations evaluated included triangular baffles, rectangular baffles, and swirler inserts. The experimental approach adhered to the "smaller-the-better" (SB) criterion for all response variables. The input parameters applied in the study are summarized in Table 1.

Table 1 Input parameters and their respective levels

S/N	Parameter	Units	Level 1	Level 2	Level 3
1	Average solar radiation (SR)	W/m^2	810	830	850
2	Average ambient temperature (T_{am})	℃	27	30	33
3	Average inlet temperature (T_{in})	℃	40	41	42
4	Type of configuration (Type-C)	-	RB	TB	SW

2.2.5. Economic analysis and feasibility study

To evaluate the feasibility of the developed drying system, an economic analysis was conducted using key financial indicators, including Net Present Value (NPV), Payback Period, and Benefit-Cost Ratio (BCR). These metrics provide a comprehensive assessment of the system's profitability, investment recovery time, and overall cost-effectiveness.

3. RESULTS

This chapter presents the most important results obtained from the experimentation and their discussions.

3.1. Evaluation of the drying system

The experiments, conducted in August 2024 at MATE University, Gödöllő, Hungary, assessed two solar air collectors with identical dimensions but different drying chambers shapes.

3.1.1. Efficiency of the solar air heaters and drying system

The efficiency of the solar air heater and corresponding dryer is shown in Fig. 4(a) and (b) respectively. The stated Figs. 4(a) and (b) illustrate a clear trend of increasing efficiency as solar radiation intensifies from the morning to midday, with the solar air heater achieving its peak efficiency and the dryers around noon. After this peak, the efficiency gradually declines as solar radiation decreases in the afternoon. This pattern emphasizes the crucial role of solar intensity, which serves as the primary factor influencing the solar drying system efficiency.

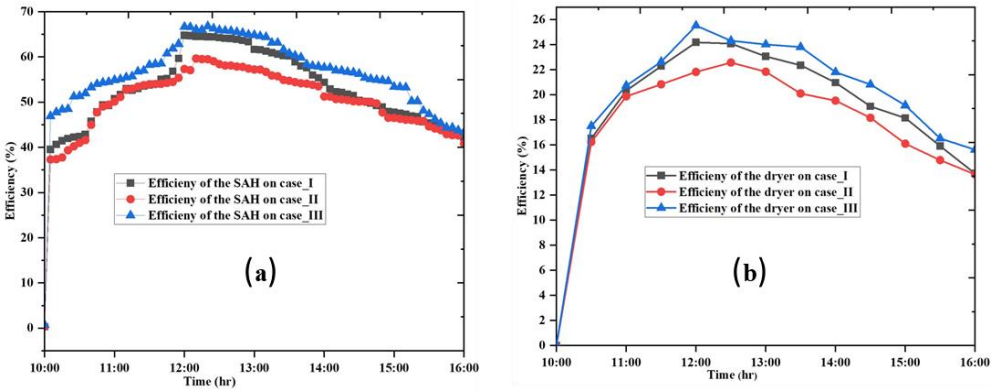

Fig. 4. Thermal efficiency of the solar air heater (a) and dryer (b)

3.1.2. SHE and SMER

To calculate the specific moisture extraction rate (SMER) and specific heat energy consumption (SHE), were evaluated both dryers under full and half-capacity conditions. In general, the energy consumption and moisture extraction rate are indirectly related, as shown in Fig. 5.

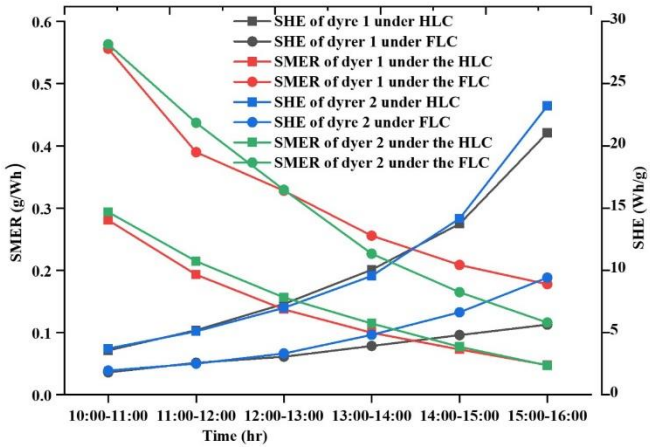

Fig. 5. Variation of the specific moisture extraction rate (SMER) and specific heat energy consumption (SHE) with time

3.2. Exergy analysis of drying system

Assessing the exergy analysis of the drying system is crucial for optimizing system design and enhancing the efficiency of solar air heaters. This section presents the experimental results evaluating the exergy performance of key components, including the solar air heaters, drying chambers, and trays.

3.2.1. Exergy analysis of solar air heaters

The exergy inflow for both solar air heaters over the two days are depicted in Fig. 6(a). The data demonstrates typical behaviour for solar air heaters, with the highest exergy inflows occurring when solar radiation is at its peak during midday, followed by a gradual decline as radiation decreases in the afternoon. This pattern is consistent with the behaviour of solar radiation, which peaks at midday and diminishes in the late afternoon. For day 1, the average efficiency of SAH_1 was 378.1743 W, while SAH_2 recorded 377.2133 W on day 1. On day 2, SAH_1 had an average exergy inflow of 376.7432 W, whereas SAH_2 showed 375.603 W. These results suggest that day 1 provided more favourable conditions for both solar air heaters (SAHs), possibly due to better solar irradiance. Similarly, the exergy outflows for both *SAHs* follow the same trend as the inflows as shown in Fig. 6(b).

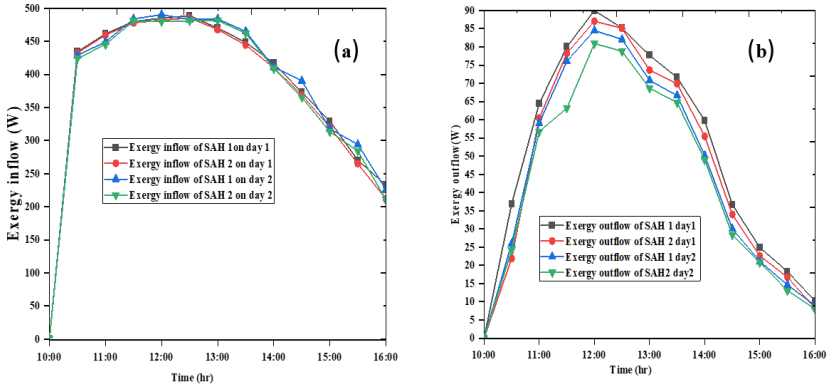

Fig. 6. Exergy inflow of (a) and exergy outflow (b) of the solar air heater

3.2.2. Exergy analysis of the drying chambers

Fig. 7 illustrates the temporal variation of exergy inflows and outflows for both dryers. This analysis provides important insights into how energy is being utilized and lost throughout the day, offering potential areas for improving dryer performance and energy efficiency. On day 1, dryer 1 had an average exergy inflow of 17.62 W, and dryer 2 has 16.74 W. The average exergy outflows were 4.44 W for dryer 1 and 3.54 W for dryer 2, with both dryers peaking at noon before decreasing towards the end of the day.

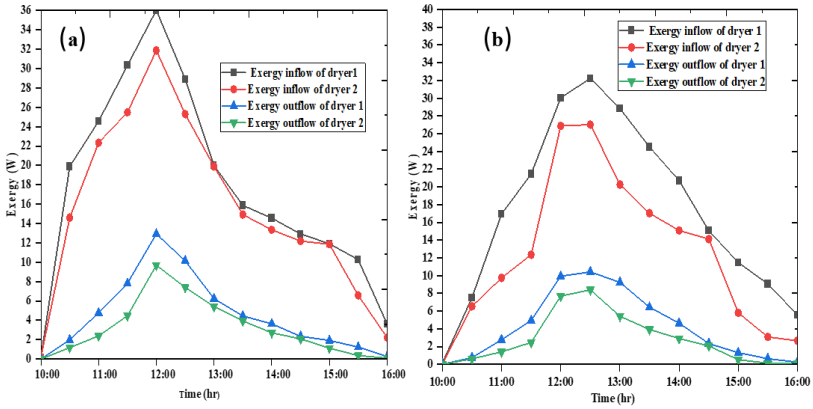

Fig. 7. Exergy analysis of the drying chambers: day1 (a) and day 2 (b)

3.2.3. Exergy assessment of the trays

Exergy inflow of the trays

The exergy inflow of the trays for both days is shown in Fig. 8. As shown in the indicated Figures, the exergy inflow in both days and both dryers demonstrate significant variations over time. The exergy flow of tray 1 consistently exhibits the highest exergy values, indicating it is the most efficient or possesses the highest beneficial work potential among the four

systems analysed. In contrast, tray 4 shows the lowest exergy inflow values, suggesting it is the least efficient in terms of useful work output. Both dryers follow expected thermal trends with peak efficiency around midday and decreasing exergy delivery with tray depth.

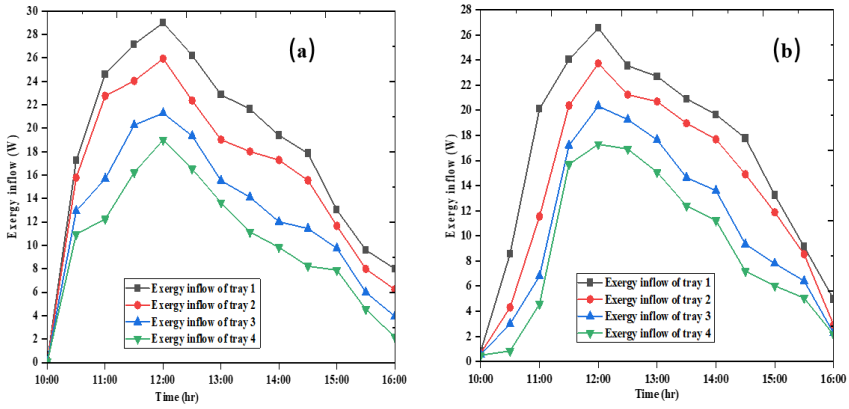

Fig. 8. Exergy inflow of the trays of dryer 1 (a) and dryer 2 (b) on day 1

Exergy outflow analysis of trays

The exergy outflow data of both dryer 1 and dryer 2 (see Fig. 9) exhibits clear and consistent thermal behaviour throughout the drying cycle. The average exergy outflows in dryer 1 are 8.82 W, 7.68 W, 6.56 W, and 5.05 W for trays bottom tray through top tray, respectively. In comparison, dryer 2 has average outflows of 7.51 W (tray 1), 6.66 W (tray 2), 5.77 W (tray 3), and 4.89 W (tray 4). These findings are crucial for optimizing dryer performance, particularly in balancing airflow, improving energy distribution to lower trays, and maximizing drying efficiency across.

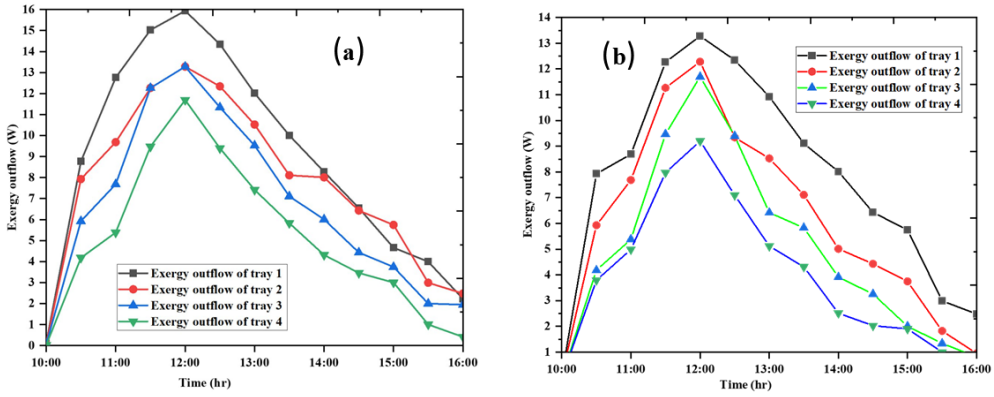

Fig. 9. Exergy outflow of the trays of dryer 1(a) and dryer 2 (b)

3.3. Drying characteristics of golden apple

3.3.1. Moisture content analysis

For the half-load capacity, the final moisture content of the apple in dryer was 6.3%, while in dryer 2, it was 9.22%. In the case of full-load capacity, the final moisture content in dryer 1 was 10.8%, and in dryer 2, it was 11.64%, achieved within 6 hours as depicted in Fig. 10. Thus, dryer 1 demonstrated a higher moisture extraction rate in both cases. Moreover, as the loading capacity decreases, the rate of moisture extraction increases. Therefore, the full capacity is more effective at moisture removal, with both dryers achieving lower final mass and moisture content compared to half capacity.

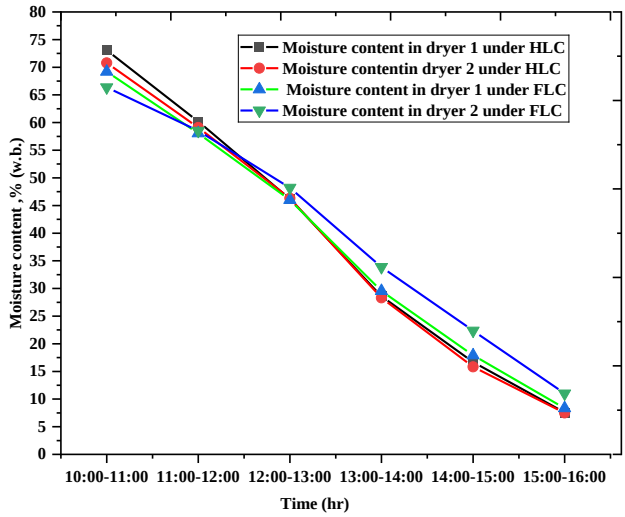

Fig. 10. Moisture content changes

3.3.2. Moisture ratio and drying curve investigation

The moisture ratio and drying curve of the sample under both half and full-capacity conditions are depicted in Fig. 11(a) and Fig. 11(b), respectively. The moisture ratio (MR) decreases over time for all conditions, indicating the effectiveness of the drying process in reducing moisture content. The drying curves for both dryer one and dryer two under half and full capacity occur under a falling rate period.

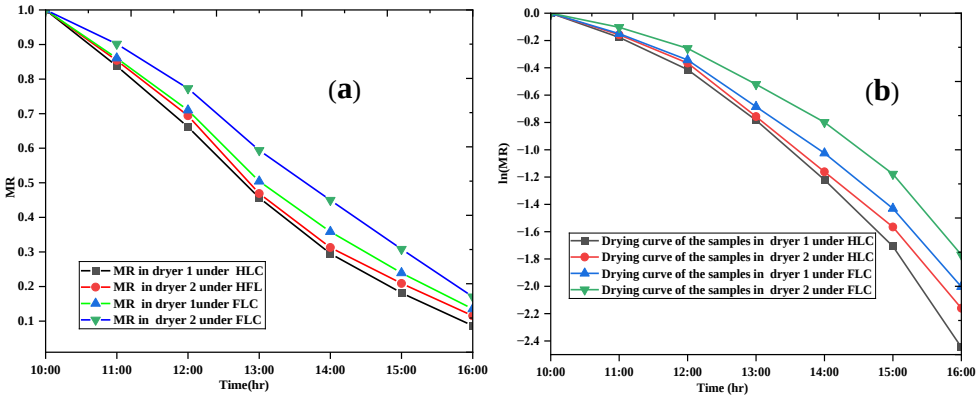

Fig. 11. Moisture ratio (a) and drying curve of the apple samples (b)

3.3.3. Selecting the best-fitting model

Ten drying models were employed to investigate the drying behaviour of apple slices and to identify the models that best describe and predict the thin-layer drying characteristics. Among these, the Midilli and Kucuk (2003) model exhibited the highest performance, achieving an R^2 value of 0.9956, an *RMSE* of 0.0321, and a χ^2 value of 0.1010, indicating its high reliability and accuracy. Additionally, the two-term and logarithmic models also demonstrated strong predictive capabilities. Across both drying days and conditions, the results were consistent, with minimal differences in statistical parameters typically involving only fractional decimal variations.

3.4. Enhancement of the drying uniformity

3.4.1. Effect of integrating triangular baffles

The temperature distribution with triangular baffles is significantly more uniform compared to without baffles, as depicted in Fig. 12. In the case of triangular baffles, the temperature differences range from 1.0 to 3.3 °C, indicating a relatively uniform distribution across the trays. On the other hand, without the triangular baffles, the temperature differences are much more significant, ranging from 3.8 to 7.6 °C, which suggests a less uniform distribution. This demonstrates that the presence of triangular baffles helps to improve heat distribution by reducing temperature gradients, resulting in a more uniform temperature profile across the trays.

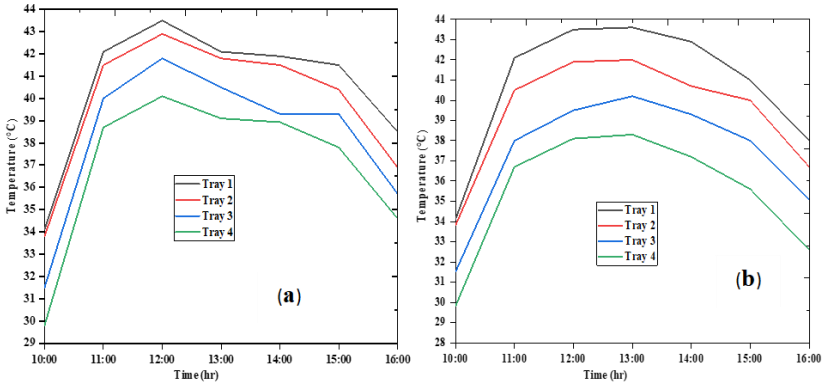

Fig. 12. Temperature distribution with triangular baffles (a) and without triangular baffles (b)

3.4.2. Effect of rectangular baffles

The temperature distribution with rectangular baffles shows generally uniform results, as illustrated in Fig. 13, with temperature differences ranging from 1.2 to 6.8 °C. The most significant variation occurs at the beginning of the day, but this difference progressively decreases as the day continues. In contrast, without rectangular baffles, the temperature differences are more significant, ranging from 4.2 to 8.7 °C, indicating a less uniform distribution. Overall, the temperature distribution with rectangular baffles is more uniform compared to those without them.

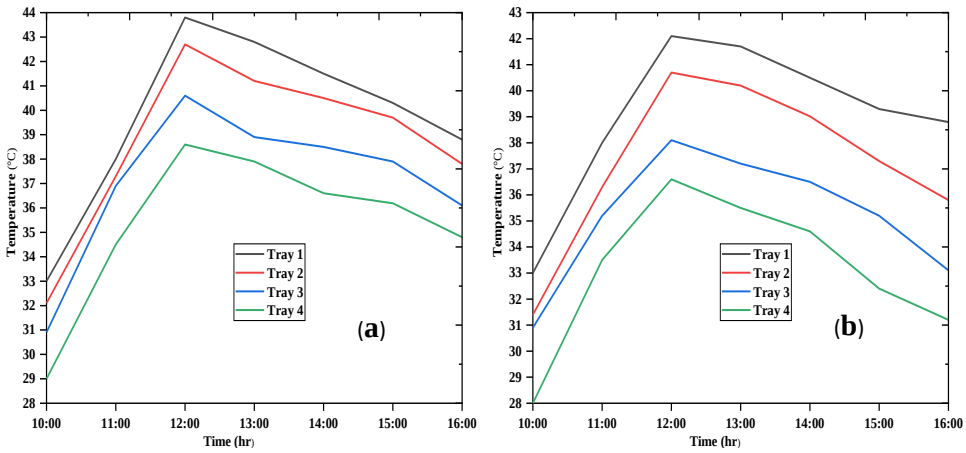

Fig. 13. Temperature distribution with rectangular baffles (a) and without rectangular baffles (b)

3.4.3. Effect of swirler

The temperature distribution with the swirler shows a generally uniform pattern (see Fig. 14), with temperature differences ranging from 2.0 to 4.8 °C. In contrast, without the swirler, the temperature differences are larger, ranging from 5.0 to 7.3 °C, indicating a less uniform distribution. In general, the temperature distribution with the swirler is more uniform than without it, as the temperature differences are consistently more minor, demonstrating that the swirler enhances heat distribution, reduces temperature gradients, and promotes better thermal uniformity across the trays.

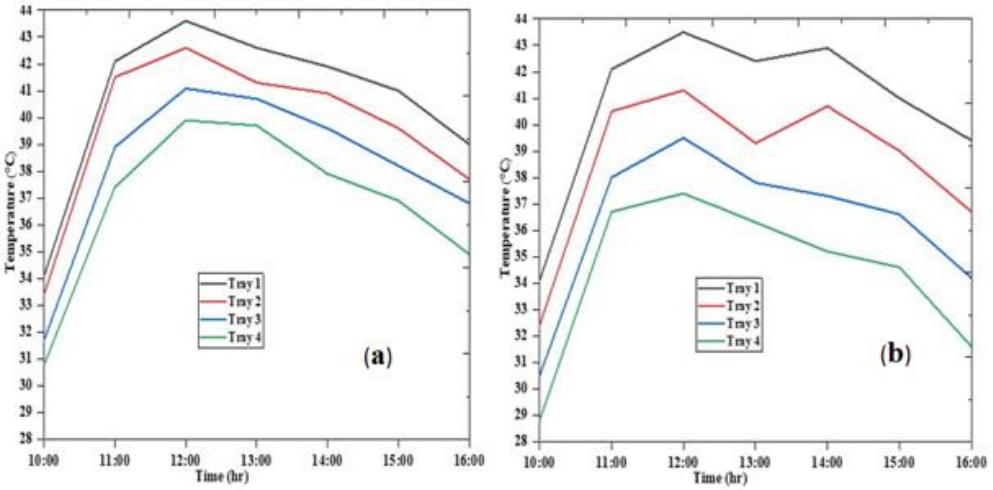

Fig. 14. Temperature distribution with swirler (a) and without swirler (b**)**

3.5. Effect of tray spacing

This study examined the impact of varying tray spacing (10 cm, 20 cm, and 30 cm) and tray arrangement configurations on drying efficiency. Experimental results revealed that a 10 cm gap between tray 1 and tray 2 delivered the highest performance in terms of mass reduction and drying rate. The 20 cm gap between tray 1 and tray 3 showed slightly lower, yet strong performance. In contrast, the configuration involving tray 1 and tray 4 (30 cm gap) yielded the lowest efficiency. These findings indicate that as tray spacing increases, both drying rate and mass reduction decrease. Furthermore, an increase in the number of trays leads to reduced weight loss and overall drying efficiency compared to setups with fewer trays.

3.6. Effect different parameters

In this section, the effects of different factors on the drying system are analysed. Taguchi analysis was employed to identify the most influential factors and determine the optimal combination based on their levels.

3.6.1. Coefficient of variance as a response parameter

The Taguchi analysis highlight the effects of several factors on drying uniformity: solar radiation (SR), inlet temperature (T_{in}), ambient temperature (T_{am}), and enhancement method type (Type-C) as shown Fig. 15. Among these, inlet temperature (T_{in}) is the most influential, as its fluctuations greatly impact moisture removal rates and drying consistency. The second most important factor is the type of enhancement method (Type-C). Therefore, prioritizing the optimization of T_{in} and Type-C is key to improving drying uniformity, with SR management providing additional stability. Ambient temperature control offers only minor benefits. The optimal combination identified is *SR* level 3, T_{am} level 1, T_{in} level 1, and Type-C level 1 (RB configuration).

Fig. 15. Main effect plot using the signal-to-noise ratio for C_v

3.6.2. Pressure as response variable

Fig. 16 shows pressure drop analysis for drying uniformity methods. Thus, the result indicates solar radiation (SR) as the most influential factor, affecting temperature gradients and airflow, thus impacting pressure resistance. Inlet temperature (T_{in}) is second, essential for maintaining balanced pressure and efficiency. The enhancement method (Type-C) ranks third, where baffle and swirler design influences airflow resistance and pressure distribution. Ambient temperature (T_{am}) has minimal effect. The optimal settings are *SR* level 2, T_{am} level 3, T_{in} level 3, and Type-C level 3.

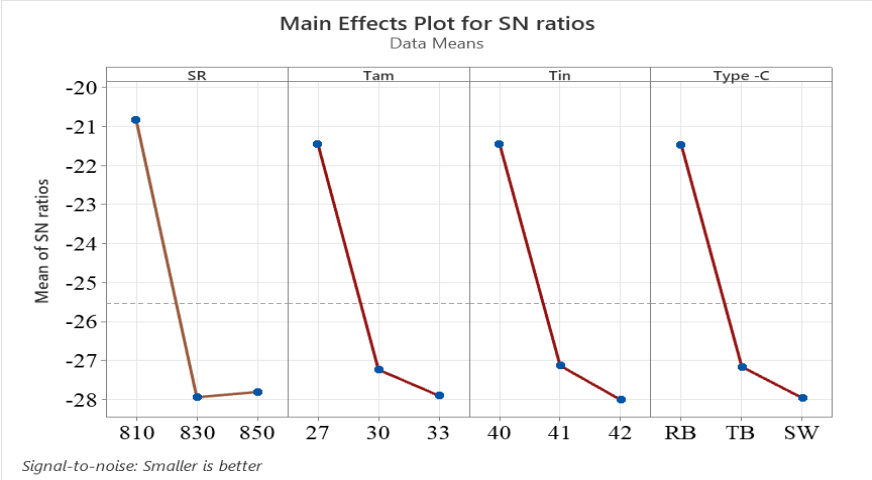

Fig. 16. Main effect plot using the signal-to-noise ratio for the pressure drop response

3.7. Feasibility study of the drying system

An economic analysis was performed to assess the feasibility of the developed drying system using key financial indicators: Net Present Value (NPV), Payback Period, and Benefit-Cost Ratio (BCR). The dryer generated a benefit of $265.88 in its first summer. The analysis revealed an NPV of $2,850.93, confirming the project's profitability. A BCR of 4.08, well above the threshold of 1, indicates strong economic viability. With a payback period of 1.73 years under two years the investment cost is recovered rapidly. Together, these results demonstrate that the developed drying system is a highly attractive and financially promising investment.

4. NEW SCIENTIFIC RESULTS

This section presents the new scientific findings from the research work as follows:

1. Improvement in drying uniformity

Based on experimental results, I enhanced the flow uniformity with the drying system using the baffles and swirlers. The addition of baffles and swirlers significantly enhances the uniformity within the drying chamber. Thus, I proved that rectangular baffles increase the drying rate and uniformity, reducing temperature gradients from 4.2 – 8.7 °C to 1.2 – 6.8 °C. Triangular baffles narrowing the temperature differences averagely from 3.8 to 7.6 °C to 1.0 – 3.3 °C. Furthermore, I proved that swirlers optimize drying uniformity across trays and improve heat distribution, reducing temperature gradients from 5.0 – 7.3 to 2.0 – 4.8 °C. The uniform airflow pattern created by the baffles and swirlers prevents localized moisture build up, ensuring that the product is evenly dried and reducing the risk of uneven drying or product degradation. These findings underscore the significance of design modifications in enhancing the performance of solar dryers, making them more effective and reliable for various applications.

2. Modelling of drying behaviour of apple slice

I have proven that the Midilli and Kucuk (2003) model (R^2 = 0.9956, *RMSE* = 0.0321, x^2 = 0.0101), the Logarithmic model (R^2 = 0.9903, *RMSE* = 0.0348, x^2 = 0.0112), and the two-term model (R^2 = 0.9944, *RMSE* = 0.0521, x^2 = 0.0266) provided best fit for the thin-layer drying behaviour of apple slices (Golden delicious), compared to other models listed out in the study. The apples were cut into cylindrical pieces with diameters ranging from 0.075 (±0.01) to 0.083 (±0.01) meters and thicknesses between 0.004 and 0.0065 (±0.001) meters. These selected models provided the most accurate predictions of moisture ratio and drying behaviour, offering robust tools for optimizing dehydration processes.

Midilli and Kucuk (2003):

$$MR = a\ exp(-k\ t^n) + b\ t.$$

The estimated coefficients and *drying constant* for the model are: a = 2.82, b = 0.0029, k = 5.02, n = 1.80 with R^2 of 0.9956.

Logarithmic:

$$MR = a\ exp(-k\ t) + c.$$

The derived model coefficients and drying constants are: a = 9.2, k = 5.29, c = 0 with R^2 of 0.9903.

Two-term:

$$MR = a\ exp(-k\ t) + b\ exp(k_1).$$

The best-fit values of coefficients and drying constants for the model are: a = 4.7, k = 3.97, b = 0.0010, k_1 = 1.0970 with R^2 of 0.9944.

3. Influence of tray spacing and number of trays

Based on the experiments conducted the number of trays and the spacing between them play a crucial role in determining the drying rate, moisture loss, and moisture ratio of the samples. These factors significantly influence heat and mass transfer during the drying process, and optimizing tray arrangements can enhance overall drying efficiency. By adjusting these parameters, it is possible to achieve more uniform moisture removal and improve the drying performance of the system. I have developed the following formulas based on tray spacing and the number of trays used, which can be applied to calculate the drying rate (DR), moisture loss (ML), and moisture ratio (MR):

$$DR = \beta_0 + \beta_1\ T_s + \beta_2\ T_n + \beta_3\ T_l + \beta_4\ (T_s\ T_n),$$

$$ML = \alpha_0 + \alpha_1\ T_s + \alpha_2\ T_n + \alpha_3\ T_l + \ \alpha_4\ (T_s\ T_n),$$

$$MR = \gamma_0 + \gamma_1\ T_s + \gamma_2\ T_n + \gamma_3\ T_l + \ \gamma_4\ (T_s\ T_l).$$

The model coefficients of correlation expressed as follows:

β_0 = 68.50, β_1 = −0.20, β_2 = −2.30, β_3 = −3.10, β_4 = 0.04 (R^2 = 0.88),

α_0 = 92.40, α_1 = −0.16, α_2 = −2.70, α_3 = −4.60, α_4 = 0.03 (R^2 = 0.85),

γ_0 = 0.95, γ_1 = −0.06, γ_2 = −0.15, γ_3 = −0.18 γ_4 = 0.01 (R^2 = 0.82).

4. Correlation solar air heater efficacy with solar irradiance, ambient temperature and outlet temperature

Based on the experimental results, I have developed a multiple linear model to estimate the relationship between the solar air heater efficiency and factors such as the amount of solar insolation received, the temperature output from the solar air heater (SAH), and the ambient temperature. The developed equation serves as a practical tool for optimizing SAH performance and can be integrated into control systems for real-time efficiency adjustments. The model was statistically validated using p-value analysis, which confirmed that

all predictors (solar insolation, ambient temperature, and SAH outlet temperature) are significant contributors to efficiency, with each coefficient yielding $p < 0.05$. The developed relation allows for performance and operational optimization of the solar air heater:

$$\eta_{sah} = \beta_0 + \beta_1 I_r + \beta_2 T_{am} + \beta_3 T_{sah,o}$$

where $\beta_0 = -31.7764$, $\beta_1 = 0.0567$, $\beta_2 = 0.7388$, $\beta_3 = 1.0123$ with $R^2 = 0.989$ and $p < 0.001$ for all parameters.

5. Correlation between dryer efficiency and the loadings

Based on the experiment conducted, I developed linear equation that relates the dryer efficiency to its loading capacity in gram. This enables users to maximize drying performance while avoiding the inefficiencies of under-loading, which wastes energy, and over-loading, which impedes airflow. For end-users, particularly farmers and small-scale operators, this correlation directly translates into energy savings by minimizing drying time and fuel consumption by applying the predicted optimal loading range. Together, these findings connect research with real-world use, offering practical strategies for efficiency of the dryer operation:

$$\eta_{dc} = \lambda L_c + b$$

$\lambda = 0.00997$, $b = 2.33$ ($R^2 = 0.99$)

where, λ defined as the ratio of the vertical change to the horizontal change, L_c represents the loading capacity of the dryer and b is the y-intercept (or constant). The estimated values of λ and b were 0.00997 and 2.33, respectively.

5. CONCLUSION AND SUGGESTIONS

The *CFD* simulation results helped in refining and optimizing the design to improve its flow behaviour. Based on the *CFD* analysis, several enhanced solar drying chamber designs were developed and evaluated using the same approach. The design that yielded the best results based on *CFD* simulations were then fabricated and subjected to experimental analysis. In the fabricated design, the impact of baffles and a swirler, which were incorporated to enhance flow and heat transfer within the chamber, was thoroughly investigated. Additionally, the drying behaviour of apple slices was studied in the newly developed solar dryer. The performance of the dryer was evaluated using energy and exergy analysis and other indicators like moisture content reduction, and drying rate of the apple slices.

To assess dryer performance, experiments were conducted under four different loading conditions: unloaded, half-capacity (250 g/tray), semi-full capacity (405 g/tray), and full-capacity (500 g/tray). The temperatures of the absorbers in the solar air heaters, along with the efficiencies of both the dryer and the solar air heaters, as well as the temperature entering the drying chamber, followed the pattern of solar radiation, peaking around midday and gradually decreasing over time. This trend highlights the direct influence of solar radiation on the thermal performance of the system, with higher radiation levels contributing to increased efficiency during the peak hours of the day.

The study evaluated the impact of flow-enhancing tools, such as baffles and swirlers, on the airflow uniformity within the solar drying system. Experimental results revealed that these modifications significantly improved thermal distribution and reduced spatial moisture variability, leading to more consistent drying performance. Statistical analysis ($p < 0.05$) confirmed that both baffles and swirlers contributed to measurable improvements in drying uniformity, with swirlers showing a marginally greater effect due to their ability to promote turbulent mixing.

Future improvements could include conducting multi-season trials to evaluate performance in varying climates, testing novel geometries like perforated plates, and exploring hybrid configurations such as baffles with angled swirlers. Investigating the synergistic effects of combined enhancements across different chamber zones and assessing post-drying product quality (colour, texture) to align with industry standards are also recommended. Additionally, exploring other flow-enhancing geometries and combination effects of multiple enhancements (e.g., baffles + swirlers) could improve results. Expanding the integration of enhancements beyond the plenum area to other chamber zones may also provide further benefits.

6. SUMMARY

MODELLING AND PERFORMANCE OPTIMIZATION OF SOLAR DRYING CHAMBER USED FOR AGRICULTURAL PRODUCTS

A comprehensive experimental analysis was carried out to enhance the drying uniformity and to mathematically model the drying behaviour of apple slices under the climatic conditions of Gödöllő, Hungary (47° 35' 39" N, 19º 21' 59" E). The primary focus of the study was on improving the performance of the solar drying chamber by incorporating flow enhancements such as baffles, a swirler, and optimized tray spacing. Additionally, the study explored the effects of varying the number of trays within the drying chamber.

To achieve the stated research objectives, experiments were conducted using three drying chambers. Two of these chambers were identical and used as benchmarks or references for comparison. The study examines the thermal efficiency of dryers, showing that higher loading capacities improve performance. Thermal efficiency increased from 12.05% at half-load to 23.50% at full-load, with higher loads enhancing heat utilization and moisture removal. However, overloading can reduce efficiency due to hindered airflow and heat distribution. Full-load operation was found to be more energy-efficient, with a better *SMER* and lower specific *SHE* compared to half-load operations. Exergy analysis revealed that peak efficiency occurred around midday when solar radiation was strongest. Lower trays in the drying chambers showed better energy retention due to their proximity to the heat source. These findings provide key insights for optimizing solar drying systems for improved energy and performance.

Among the evaluated drying models, the Midilli and Kucuk model demonstrated superior fitting performance, followed by the logarithmic model (and then the two-term model. Drying occurred primarily in the falling rate period, with no distinct constant-rate phase.

Adding the baffles significantly improved air flow uniformity and moisture removal. Taguchi analysis confirmed that solar irradiance and inlet temperature were the dominant factors governing drying uniformity. Collectively, these enhancements substantively mitigate non-uniform drying, underscoring their potential to advance solar dryer design for industrial and agricultural applications. Based on the economic indicators used, the project is profitable and feasible.

7. MOST IMPORTANT PUBLICATIONS RELATED TO THE THESIS

Refereed papers in foreign languages:

1. Halefom, K., Buzas, J., Farkas, I. (2021): Modelling and simulation of air flow on the surface of solar air heater using computational fluid dynamics, R&D in Mechanical Engineering Letters, Vol. 21, pp. 78–84.
2. Kidane, H., Buzas, J., Farkas, I. (2023): Airflow optimization of solar drying unit using computational fluid dynamics approach, Mechanical Engineering Letters, Vol. 24, pp. 52–74.
3. Kidane, H., Buzas, J., Farkas, I. (2023): Computational analysis of horizontally and inclined finned solar air collector, Jurnal Tekno Insentif, Vol. 17, pp. 150–159. https://doi.org/10.36787/jti.v17i2.1172
4. Kidane, H., Farkas, I., Buzás, J. (2024): Assessing the carrying capacity of solar dryers applied for agricultural products: a systematic review, Discover Energy, Vol. 4, 6. https://doi.org/10.1007/s43937-024-00031-x
5. Kidane, H., Farkas, I., Buzás, J. (2025): Mathematical modelling of golden apple drying and performance evaluation of solar drying systems using energy and exergy approach, Scientific Reports, Vol. 15(1), 7805. https://doi.org/10.1038/s41598-025-92133-2. (Scopus: Q1 IF: 3.8)
6. Kidane, H., Farkas, I., Buzás, J. (2025): Characterizing agricultural product drying in solar systems using thin-layer drying models: comprehensive review, Discover Food, Vol. 5(1), 84. https://doi.org/10.1007/s44187-025-00362-1. (Scopus: Q1, IF: 4.1)
7. Kidane, H., Farkas, I., Buzás, J. (2025): Performance Evaluation of Solar Drying Chambers and Drying Kinetics of Apple Slices, Energy Reports, Vol. 13, pp. 4528–4540. https://doi.org/10.1016/j.egyr.2025.04.016. (Scopus: Q1, IF: 4.7)
8. Kidane, H., Farkas, I., Buzás, J. (2025): Role of computational fluid dynamics in solar air heating: a comprehensive overview of applications, benefits and future directions, Journal of Thermal Analysis and Calorimetry. https://doi.org/10.1007/s10973-025-14261-1. (WoS: Q2, IF: 3.0)
9. Kidane, H., Farkas, I., Buzás, J. (2025): Modeling Airflow Dynamics in Solar Drying Chambers: A Comprehensive Review of CFD Applications, Discover Applied Sciences https://doi.org/10.1007/s42452-025-06894-6. (Scopus: Q2)
10. Kidane, H., Farkas, I., Buzás, J. (2025): Optimizing solar drying chamber performance: Taguchi analysis of uniformity enhancement methods, International Journal of Energy Research, https://doi.org/10.1155/er/5061778. (Scopus Q2, IF: 4.3).

11. Kidane, H., Farkas, I., Buzás, J. (2025): Design, Fabrication and Performance Evaluation of Solar Drying Chamber Used for Apple Slices, Acta Technologica Agriculturae, Vol. xx(xx), pp. xxx. https://doi.org/xxxxx/xxxxxx (Scopus: Q3, IF: 1.3) (Accepted)
12. Kidane, H., Farkas, I., Buzás, J. (2025): Enhancing the drying uniformity in solar drying systems: computational and experimental study, International Journal of Thermofluids, Vol. xx(xx), pp. xxx. https://doi.org/xxxxx/xxxxxx (Scopus: D1) (in Progress)

Refereed papers in Hungarian language

13. Buzás, J., Halefom, K., Farkas, I. (2022): Napenergiás szárítók áramlástani vizsgálata, Mezőgazdasági Technika, Vol. 18, pp. 2–5.